Volume 24 (1) 2025

Page 35 - 44

Mekanika: Majalah Ilmiah Mekanika

Masonry Wall Performance Estimation Under Blast Loading: A Study Using Finite Element Analysis

Siti Nurlita Fitri[1*], Muhammad Arif Husni Mubarok[2], Halim Hamadi[3,4], Quang Thang Do[5], Afiq Azfar Pratama[6], Rommy Rommy[6]

1 Department of Civil Engineering, Gifu University, Gifu, Japan
2 Department of Research and Development, P.T. Dimonitor Indonesia Sejahtera, Surakarta, Indonesia
3 Tomsk Polytechnic University, Tomsk Oblast, Russia
4 Department of Electro Instrumentation, Polytechnic Institute of Nuclear Technology, Yogyakarta, Indonesia
5 Department of Naval Architecture and Ocean Engineering, Nha Trang University, Nha Trang, Viet Nam
6 Research Center of Nuclear Materials and Radioactive Waste Technology, National Research and Innovation Agency (BRIN), Tangerang Selatan, Indonesia

*Corresponding Author's email address: siti.nurlita.fitri.d4@s.gifu-u.ac.jp

Keywords:
Masonry wall
Blast load
Dynamic response
Finite element method

Abstract
This paper studies the dynamic response of masonry wall structures under blast loading. It requires a detailed understanding of the explosion phenomenon, wave propagation, and the structure's response to these shocks. The blast load is applied to the surface of the masonry wall. The main focus is to evaluate the dynamic response of a masonry wall due to a blast load. We used the Finite Element Method (FEM) for modeling the dynamic structural response to explosions. The explicit finite element modeling and analysis are done using ABAQUS CAE software. In this study, the model uses materials, namely Masonry. Masonry could be a composite structure entrenched by blocks of bricks articulated by mortar joints. In this study, the properties of the material used are clay bricks masonry as orthotropic materials. The structural analysis carried out in this study is related to stress, strain, and deformation due to the given loading.

1 Introduction

The masonry walls are the parts that support the building. The analysis of the masonry wall structure and its behavior toward explosions attracted significant scientific research [1,2]. Explosions may be helpful or dangerous to human life. Practical explosions extract particles from rocks, destroy deserted buildings, etc [3]. These days, however, explosions have come to be instruments to destroy human lives in addition to public and non-public property [4]. The explosion's loading can cause substantial harm to structural parts similar to columns and plates [5]. The vehicle response to the explosion load is troublesome to predict as several variables are involved, such as the plate angle, position and form of the payload, and so on [6]. Therefore, planning of blast-protective buildings is crucial. As a result, it is the sole means of quality in many combat situations [7]. To ensure efficient and safe wall design, it is essential to identify and optimize key design parameters [8]. The ability of the wall material to resist significant deformation before breaking may be a key criterion in structural applications [9].

https://dx.doi.org/10.20961/mekanika.v24i1.97153

Revised 17 March 2025; received in revised version 20 March 2025; Accepted 21 March 2025
Available Online 31 March 2025

2579-3144

The abrupt unloading of energy related to Weapon of Mass Destruction (WMD) explosions results in the generation of shock waves and the formation of highly regarded and hard-hitting gas bubbles within the close water [10]. The sort and extent of harm depends on whether or not the explosion has occurred in grips with the target or nearby [11]. This paper aims to grasp the dynamic response of wall structures to the loading of explosions. Blast pressure is calculated to be an exponential kind of negativity in time. The structure is perfect as a multi-degree system of freedom, and the equations that govern motion are often established by the tactic of parts up to and balance of forces. Dynamic analysis is considered by plate cracking behavior once the utmost moment of elastic plate component is capable of a critical moment [12]. The masonry wall can be seen in Figure 1.

Figure 1. Masonry wall and building process example

2 Materials and Methods

Masonry could be a complicated material consisting of flat bricks and mortar. There are two other ways to research masonry. The primary method is a separate method in which every material is considered individually, alongside its distinctive physical and geometric properties. During this method, further attention ought to be paid to the outline of contacts between phases [13,14]. This approach is commonly verified in laboratory tests for static and dynamic loads [15]. However, because of the dearly won computing requirements, it is a severe limitation in analysis, even for comparatively small specimens [16,17]. The second approach regards the structure as continuous; the heterogeneous brick structure is replaced with homogenized masonry. An identical approach considers the modelling of metallic element micro-cracks conferred in [18]. An explosion occurs when a large amount of potential energy is rapidly released into the surrounding environment. Commonly, the force of explosions is measured using overpressure and dynamic pressure terms. Overpressure can be defined as a rapid increase of pressure above ambient pressure. Dynamic pressure can be defined as the force exerted by the shock wave of an explosion as it moves through the air, so dynamic pressure has a strong relation with the speed and density of the shock wave. During the explosion, the blast wave rapidly increases pressure above the atmospheric pressure. This pressure gradually decreases as the shock waves move away from the detonation point; this pressure will drop below ambient pressure quickly and create a negative phase. After the arrival time of the explosion, the pressure rapidly increases until it reaches the peak value of overpressure. Then, the pressure gradually decreases during the Duration of Time (*td*) and still decreases until a partial vacuum/negative phase has been generated. This peak pressure can be defined as Equation 1 below.

$$P = K[\frac{m}{r^3}] \tag{1}$$

Blast loads are sometimes divided into loads due to shock and dynamic pressure. Because the front shock waves are reflected, the hydrodynamic pressure behind the front is doubled, usually expressed as overpressure [19]. Dynamics are caused by particle velocity or atmospheric displacement pressure [4]. The function of scale distance and explosive equivalent mass, presented in Equation 2, significantly affects various blast parameters such as peak pressure and impulse, duration of positive and negative phases, and arrival time.

$$Z = \frac{R}{W^{\frac{1}{3}}} \tag{2}$$

Where, (R) is the actual effective distance from the explosion. (W) is mainly expressed in kilograms [20]. During an air blast overpressure, two types of overpressures happen, namely incident overpressure (P_{io}) and reflected overpressure (P_{ro}). Incident overpressure can be defined as initial pressure that travels through the air directly from the detonation point, while reflected overpressure is greatly affected by surroundings such as ground, walls, or another obstacle. The total air blast overpressure (P_{total}) magnitude can be defined as a function of these two parameters and the incident angle (θ), which can be presented in Equations 3-5.

$$P_{total} = \begin{cases} [P_{ro}(t) - 2P_{io}(t)\cos\theta^2 + [\cos\theta + 1]P_{io}(t), \cos\theta \geq 0,] \\ P_{io}(t), \cos\theta < 0 \end{cases} \tag{3}$$

$$P_{io} = (P_{so} - P_a)\left(1 - \frac{t-t_a}{t_0}\right) e^{-\left(\beta\frac{t-t_a}{t_0}\right)} \tag{4}$$

$$P_{ro}(t) = 2P_{io}(t) + \frac{(\gamma+1)\{P_{io}(t)\}^2}{2\gamma P_a + (\gamma-1)P(t)} \tag{5}$$

Where, (t_a) represents the arrival time of the blast towards the target surface and (γ) is the ratio of the specific heat of air. To get the parameters of the explosion load used the help of graphs to form the explosion function, namely Scaled distance (Z), positive phase amplitude (P_{so}), negative phase amplitude ($P_{so}-$), linear positive phase duration (t_{of}), positive phase duration (t_o), negative phase duration (t_o-) and linear negative phase duration ($t_{of}-$) [21]. The time evolution of the reflected pressure is modelled with the well-established modified Friedlander equation can be seen in Equations 6 and 7.

$$(t) = P_{SO}\,(1 - \frac{t}{t_0})\ \exp\,(-d\,\frac{t}{t_0}) \tag{6}$$

Where, ($P(t)$) is the pressure at time (kPa); (P_{so}) is the peak incident pressure (kPa); (t_0) is the positive phase duration (ms); (d) is the wave decay coefficient.

$$i = \int_{t_a}^{t_0} P(t)\, dt \tag{7}$$

where, (t_a) is the arrival time (ms).

This study used the Finite Element Method (FEM) to determine masonry wall response to blast loads to find stress, strains, and displacements. Stress analysis using the Finite Element Method (FEM) can determine the critical point that has the highest stress. This critical point is one of the factors that can cause fatigue failure [22]. The benefits of using Computer Aided Design (CAD) / Computer Aided Engineering (CAE) technology for mechanical layout, electrical, and fuel systems for rapid analysis with system configuration and reconfiguration were also realized [23]. Stress is the intensity of the internal force on the structural element as a reaction to the deformation that occurs due to the external load's operation. In this study, the magnitude given is 1. When deformation occurs, the object will also have various stresses and strains at each point, influenced by factors such as the material's properties, the direction of the applied force, and the structure's shape. Different regions may experience tensile, compressive, or shear stress, and the distribution of these stresses plays a crucial role in determining the overall structural response to the applied load. In this work, the Von Mises stress is considered as presented in Equation 8. Strain is material deformation or displacement resulting from an applied stress shown in Equation 9, and deformation can be caused by several factors, including the pressure applied to the wall described in Equation 10.

$$\sigma_V = \sqrt{\frac{(\sigma_{xx} - \sigma_{yy})^2 + (\sigma_{yy} - \sigma_{zz})^2 + (\sigma_{zz} - \sigma_{xx})^2 + 6(\sigma_{xy}^2 + \sigma_{yz}^2 + \sigma_{zx}^2)}{2}} \tag{8}$$

$$\varepsilon = \frac{\Delta l}{l_0} \tag{9}$$

$$D = X_f - X_i \tag{10}$$

In this study, the dimension size is varied. This design and simulation used three variations of thickness size: 2.15E-01, 4.30E-01, and 8.60E-01. We also varied the shape, including flat and curved. The design can be seen in Figures 2 and 3.

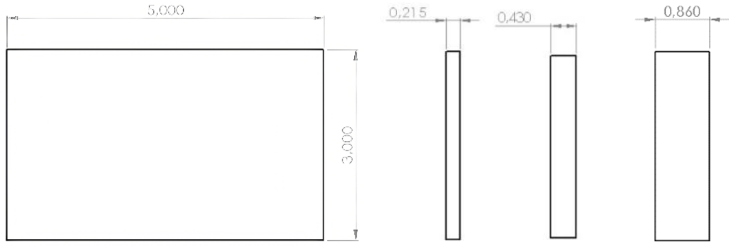

Figure 2. Dimension flat masonry wall variation models

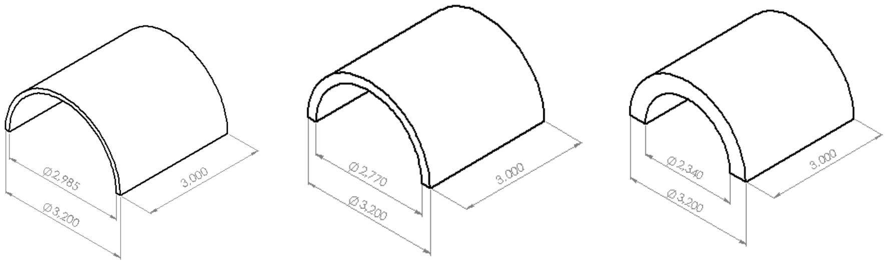

Figure 3. Dimension barrel masonry wall variation models

Relative errors of the natural periods are negligible when meshing the area is smooth. The mesh size is shaped uniquely and dictated by the software system, which automatically adjusts to the complexity of the structure and the computational capabilities of the system being used. During this design and simulation process, three variations of mesh size were utilized: 4.00E-02, 8.00E-02, and 1.20E-01. These mesh sizes were selected to explore the effects of different detail levels on the results accuracy and computational efficiency. Smaller mesh sizes typically provide higher accuracy but demand more significant computational resources and longer processing times. In contrast, larger mesh sizes are more computationally efficient but may sacrifice precision in regions with intricate details or high stress and strain gradients. The mesh shape and distribution for each variation can be seen in Figure 4, which illustrates how the software accommodates the complexity of the frame design by refining or coarsening the mesh, accordingly. A set of boundary conditions is applied on the model's edge to restrict its translation and rotational movements during and after blast.

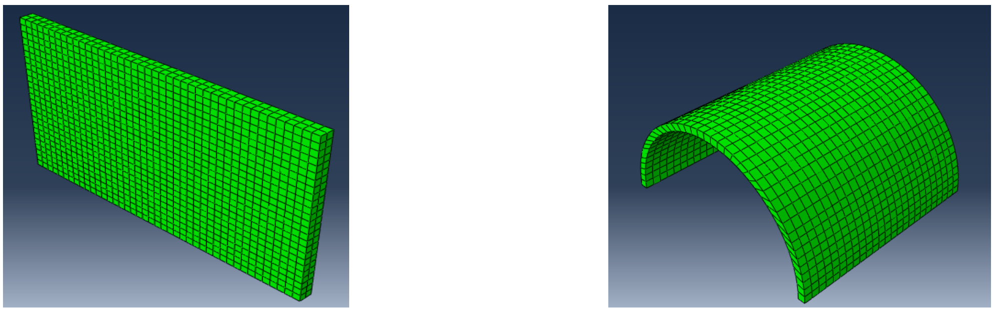

(a) (b)

Figure 4. Mesh variation models: (a) Flat masonry wall, and (b) Barrel masonry wall

In this study, the model uses materials, namely simplified masonry, which could be a composite structure entrenched by blocks of bricks articulated by mortar joints. The properties of the materials used are clay bricks and masonry as orthotropic materials. Therefore, to characterize the assorted structural effects of explosions, a coupled numerical approach exploiting Lagrangian and Eulerian strategies is adopted to analyze the response of masonry walls [1]. The material properties can be seen in Table 1.

Table 1. Material properties

Density (kg/m^3)	Young Modulus (MPa)	Poisson Ratio
2.00E+03	11.8E+9	1.50E-01

In this work, ignition refers to initiating combustion or a rapid chemical reaction, often involving flammable materials, by providing the necessary energy to start the process. There are many potential ignition sources; the most likely source will depend on the specific scenario and the materials involved. Ignition of blast load on the material is defined using the time/frequency in units of milliseconds and amplitude in units of pascals, as shown in Table 2. The plot amplitude is shown in Figure 5.

Table 2. Amplitude data

Time / Frequency (ms)	Amplitude (Pa)
0	1021250
0.01	0

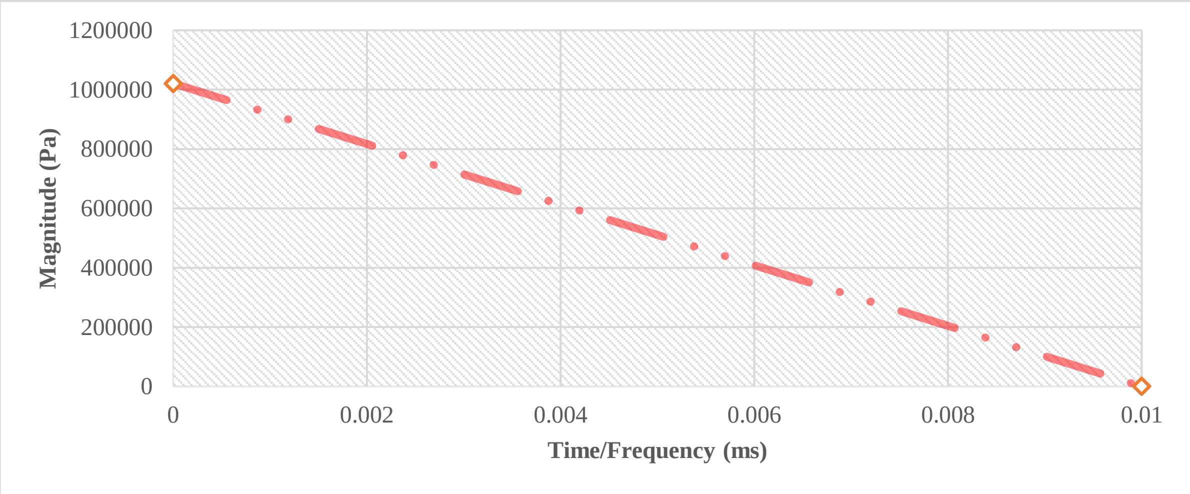

Figure 5. Amplitude plot

3 Results and Discussion

Tables 2 and 3 show the results of simulations on design variations, Von Mises stress, strain, and displacement.

. **Table 3.** Flat masonry wall simulation result

Thickness (mm)	Mesh	Von Mises Stress (N/mm^2)		Strain		Displacement (mm)	
		Min	Max	Min	Max	Min	Max
2.15E-01	4.00E-02	1.50E+05	1.81E+07	2.98E-06	1.52E-03	0.00E+00	6.31E-03
	8.00E-02	4.17E+05	1.68E+07	1.00E-05	1.52E-03	0.00E+00	8.27E-03
	1.20E-01	8.33E+05	2.19E+07	2.01E-05	1.97E-03	0.00E+00	1.36E-02
4.30E-01	4.00E-02	4.47E+04	3.77E+06	3.43E-07	3.43E-04	0.00E+00	3.16E-04
	8.00E-02	1.08E+05	2.62E+06	2.21E-06	2.31E-04	0.00E+00	4.21E-04
	1.20E-01	9.55E+04	2.71E+06	1.31E-06	2.41E-04	0.00E+00	5.33E-04
8.60E-01	4.00E-02	2.44E+04	7.40E+06	3.62E-06	6.76E-04	0.00E+00	6.48E-04
	8.00E-02	4.32E+04	5.88E+06	7.12E-06	5.37E-04	0.00E+00	6.43E-04
	1.20E-01	4.79E+04	5.28E+06	8.94E-07	4.44E-04	0.00E+00	6.50E-04

Table 4. Barrel masonry wall simulation result

Thickness (mm)	Mesh	Von Mises Stress (N/mm^2)		Strain		Displacement (mm)	
		Min	Max	Min	Max	Min	Max
	4.00E-02	2.25E+05	2.50E+07	6.91E-06	1.54E-03	0.00E+00	3.14E-03
2.15E-01	8.00E-02	5.91E+05	1.41E+07	5.36E-06	3.30E-04	0.00E+00	4.81E-03
	1.20E-01	7.80E+05	1.40E+07	1.30E-05	2.39E-04	0.00E+00	4.12E-03
	4.00E-02	8.59E+04	1.40E+07	1.34E-06	3.98E-04	0.00E+00	1.77E-03
4.30E-01	8.00E-02	2.04E+05	1.28E+07	7.57E-06	4.97E-04	0.00E+00	1.74E-03
	1.20E-01	1.37E+05	1.03E+07	8.34E-06	6.10E-04	0.00E+00	1.50E-03
	4.00E-02	3.37E+04	6.56E+06	8.94E-07	5.98E-04	0.00E+00	4.64E-04
8.60E-01	8.00E-02	4.65E+04	4.67E+06	2.09E-07	4.21E-04	0.00E+00	4.42E-04
	1.20E-01	5.08E+04	4.03E+06	7.15E-07	3.57E-04	0.00E+00	4.34E-04

The results of the Von Mises stress analysis show a range of values on the flat masonry wall. The lowest stress recorded is 2.44E+04 N/mm² at a deformation of 8.60E-01 mm with a mesh size of 4.00E-02. In contrast, the highest stress is 1.81E+07 N/mm² at a deformation of 2.15E-01 mm, also using a 4.00E-02 mesh. These variations indicate significant differences in stress concentration depending on the deformation and mesh refinement. Regions experiencing higher stress are more likely to fail or require reinforcement. The detailed stress distribution and critical points can be seen in Figure 6, providing insight into the structural behavior under load.

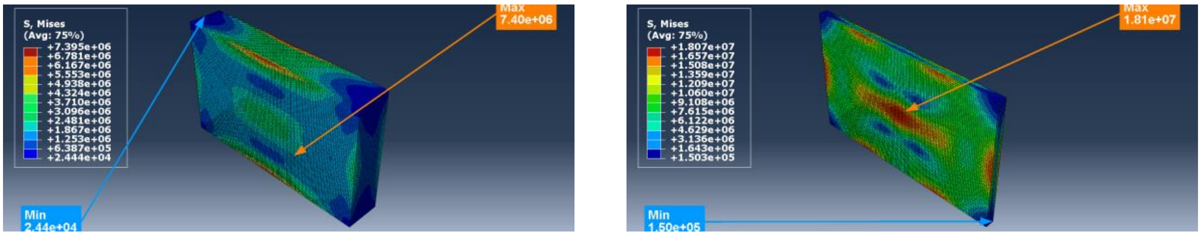

(a) (b)

Figure 6. Von Mises stress of the flat masonry wall: (a) Min value, and (b) Max value

The strain analysis results show a range of values on the flat masonry wall. The lowest strain recorded is 3.73E-07 at a deformation of 4.30E-01 mm with a mesh size of 4.00E-02. In contrast, the highest strain is 1.97E-03 at a deformation of 2.15E-01 mm with a coarser mesh size of 1.20E-01. These variations highlight how strain distribution is influenced by mesh refinement and deformation levels.

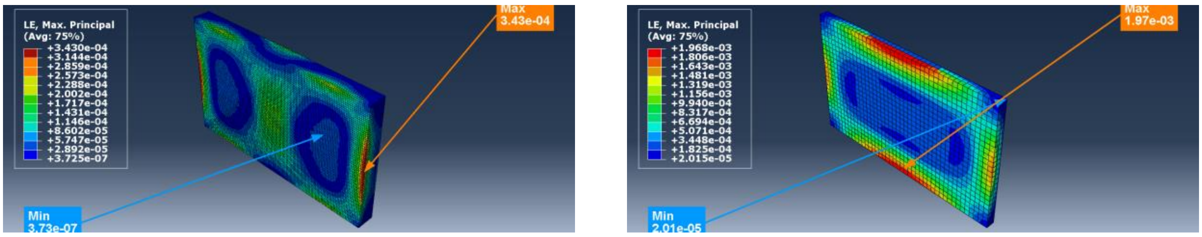

(a) (b)

Figure 7. Strain of the flat masonry wall: (a) Min value, and (b) Max value

The result of displacement is that the lowest value is 0.00E+00 mm on the flat masonry wall 2.15E-01 mm with 1.20E-01 mesh, and the highest value is 1.36E-02 mm on the flat masonry wall 2.15E-01 mm with 1.20E-01 mesh. The results can be seen in Figure 8.

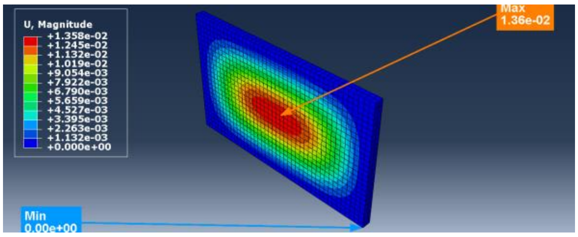

Figure 8. Displacement of the flat masonry wall

The result of Von Mises stress is that the lowest value is 3.37E+04 N/mm^2 on the barrel masonry wall 8.60E-01 mm with 4.00E-02 mesh, and the highest value is 2.50E+07 N/mm^2 on the flat masonry wall 2.15E-01 mm with 4.00E-02 mesh. The results can be seen in Figure 9.

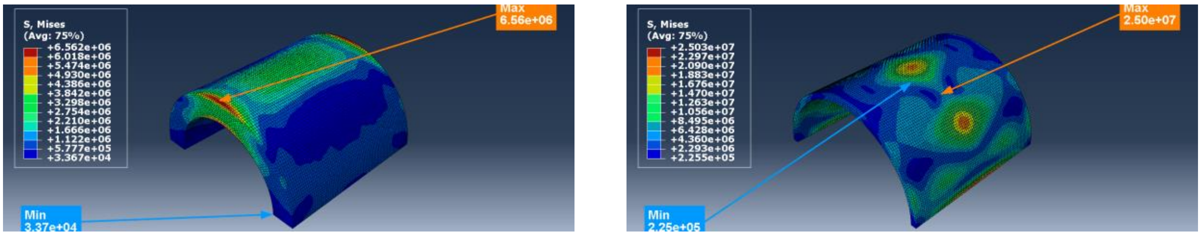

(a) (b)

Figure 9. Von Mises stress of the barrel masonry wall: (a) Min value, and (b) Max value

The results of the strain analysis show a range of values on the flat masonry wall. The lowest strain recorded is 2.09E-07 at a deformation of 8.60E-01 mm with a mesh size of 8.00E-02, as seen in Figure 10. On the other hand, the highest strain is 1.54E-03 at a deformation of 2.15E-01 mm with a finer mesh size of 4.00E-02. These results indicate how strain varies depending on the mesh size and the deformation of the wall. Finer meshes tend to provide more accurate strain values, while coarser meshes may not capture localized deformations as effectively. The results of the strain analysis show a range of values on the flat masonry wall. The lowest strain recorded is 0.00E+00 at a deformation of 2.15E-01 mm with a mesh size of 8.00E-02. In contrast, the highest strain is 4.81E-03 at the same deformation of 2.15E-01 mm with the same mesh size of 8.00E-02. These results indicate the variation in strain across different wall regions, with the highest strain occurring in certain localized areas. The strain distribution can be seen in Figure 11.

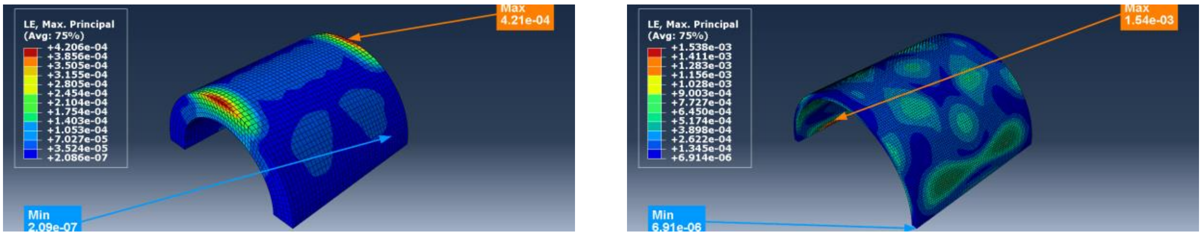

(a) (b)

Figure 10. Strain of the barrel masonry wall: (a) Min value, and (b) Max value

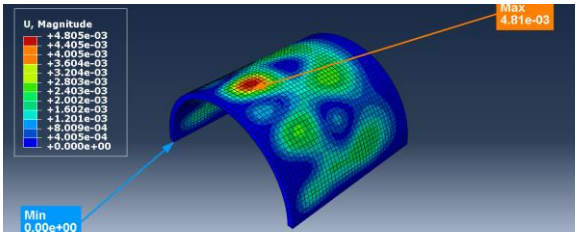

Figure 11. Strain of the barrel masonry wall

Based on the simulation results, graphs of the minimum and maximum values of strain, stress, and deformation were obtained, shown in Figures 12-14. These graphs illustrate the variation in strain, stress, and deformation across the flat masonry wall, highlighting the areas of highest and lowest values. The graphs compare the extreme values for each parameter, offering valuable insights into the structural response under the applied load conditions. The visual representation helps to identify critical zones that may require further attention or reinforcement.

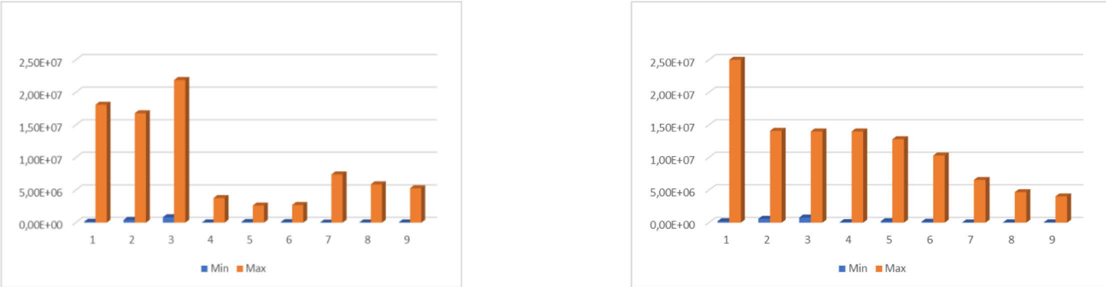

(a) (b)

Figure 12. Simulation result graph Von Mises stress: (a) Flat masonry wall, and (b) Barrel masonry wall

(a) (b)

Figure 13. Simulation result graph Von Mises stress: (a) Flat masonry wall, and (b) Barrel masonry wall

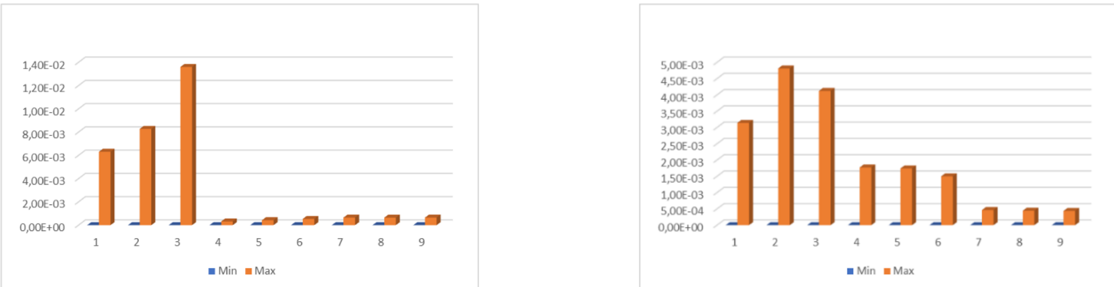

(a) (b)

Figure 14. Simulation result graph displacement: (a) Flat masonry wall, and (b) Barrel masonry wall

Structural analysis deals with stress, strain, and deformation in engineering structures. Stress is the strength of force from interactions, while strain is the resulting deformation. The increase in stress leads to an increase in the strain ratio [24]. Displacement may be a shift or displacement that happens in a given loading stress material. It helps justify the protection, particularly the development material's life, wherever the more critical the strain, the larger the displacement, the smaller the safety level, and the other way around [25]. This study's results came from 3 variations: design, thickness, and mesh. In the design, there are two variations, flat and barrel. The thickness of the benchmark wall is 2.15E-01 mm, 4.30E-01 mm, and 8.60E-01 mm. There are three variations on mesh: 4.00E-02, 8.00E-02, and 1.20E-01.

The simulation results show that the highest value of Von Mises stress is in the flat masonry wall, which has a thickness of 2.15E-01 mm and 4.00E-02 mesh, while the lowest value is in a thickness of 8.60E-01 mm and 4.00E-02 mesh. The highest value of Von Mises stress is in the barrel masonry wall, which has a thickness of 2.15E-01 mm and 4.00E-02 mesh, while the lowest value is also in a thickness of 8.60E-01 mm and 4.00E-02 mesh. In the strain, the max value found in the flat masonry wall, which has a thickness of 2.15E-01 mm and 8.00E-02 mesh, while the lowest value in the flat masonry wall, with a thickness of 4.30E-01 mm and 4.00E-02 mesh. The maximum value found in the barrel masonry wall, which has a thickness of 2.15E-01 mm and 4.00E-02 mesh, while the lowest value in the barrel masonry wall, with a thickness of 8.60E-01 mm and 8.00E-02 mesh.

In displacement, the maximum value in the flat masonry wall has a thickness of 2.15E-01 mm and 1.20E-01 mesh, while the lowest value is in the whole masonry wall. The max value in the barrel masonry wall has a thickness of 2.15E-01 mm and 8.00E-02 mesh, while the lowest value is in the whole masonry wall. This result is due to the magnitude of loading on the wall surface. The calculation results were verified experimentally at the dynamic explicit test facility. This masonry wall must undergo further examination and research to obtain adequate quality. This project can be used as a material for future consideration in building construction.

4 Conclusions

In this study, the simulation results can be seen that the highest value of Von Mises stress in the flat masonry wall, which has a thickness of 2.15E-01 mm and 4.00E-02 mesh, while the lowest value is with a thickness of 8.60E-01 mm and 4.00E-02 mesh. The highest value of Von Mises stress in the barrel masonry wall is 2.15E-01 mm and 4.00E-02 mesh, while the lowest value is 8.60E-01 mm and 4.00E-02 mesh. The max strain value in the flat masonry wall is 2.15E-01 mm and 8.00E-02 mesh, while the lowest value is with a thickness of 4.30E-01 mm and 4.00E-02 mesh. The highest strain value in the barrel masonry wall is 2.15E-01 mm and 4.00E-02 mesh, while the lowest is 8.60E-01 mm and 8.00E-02 mesh. The max value in displacement in the flat masonry wall has a thickness of 2.15E-01 mm and 1.20E-01 mesh, while the lowest value is in the all. The highest strain value is in the barrel masonry wall, which has a thickness of 2.15E-01 mm and 4.00E-02 mesh, while the lowest value is in all. The author conducted this study on the behavior of concrete masonry walls under blast. Various geometry conditions are applied. This research used a ratio of thickness and mesh to suit the needs. The key point method is recommended to help identify instability and subsequent transition modes.

References

1. J. R. Smith and L. M. Thompson, *Structural Analysis of Masonry Walls under Explosive Loads*, New York: Wiley Publishing, 2015.
2. T. Nguyen, and M. Alam, "Impact of Explosive Blasts on Masonry Structures: A Review of Experimental and Simulation Studies," *Int. J. Struct. Stab. Dyn.*, vol. 14, no. 5, pp. 2055-2069, 2020.
3. A. Williams, and P. Carter, *Explosion Effects on Civil Infrastructure: Theory and Practice*. Washington D.C: Engineering Press, 2018.
4. M. Baxani, N. Anandavalli, J. Rajasankar, S. Purohit, “Analysis of A Masonry Wall Under Blast Loads Using Coupled Lagrangian-Eulerian Method,” *in the International Conference on Advances in Civil Engineering Materials and Processes*, Hyderabad, India, 2015.
5. F. Zhang, F. Lu, and Y. Guo, "Experimental and Numerical Study on Masonry Walls under Blast Loads," *J. Perform. Construct. Facilit.*, vol. 22, no. 5, pp. 342-349, 2008.
6. T. Ngo, P. Mendis, A. Gupta, and J. Ramsay, "Blast Loading and Blast Effects on Structures – An Overview," *Electron. J. Struct. Eng.*, vol. 7, pp. 76-91, 2007.
7. Y. Shi, Z. X. Li, and H. Hao, "A New Method for Blast Load Identification on Building Structures." *Int. J. Impact Eng.*, vol. 36, no. 4, pp. 418-426, 2009.
8. K. A. Marchand, A. R. Doud, and E. B. Williamson, "Structural Response of Masonry Walls Subjected to Blast Loads." *Eng. Struct.*, vol. 32, no. 8, pp. 2345-2356, 2010.
9. A. S. Kumar, K. U. Gokul, P. V. K. Rao, and A. Jagannadham, “A Blast loading of underwater targets e-A study through Explosion Bulge Test experiments,” *Int. J. Impact Eng.*, vol. 76, pp. 189-195, 2015.

10. A. H. Keil, *The Response of Ships to Underwater Explosions*, Virginia: Structural Mechanics Laboratory Research and Development Report, 1961.
11. B. Langrand, N. Leconte, A. Menegazzi dan A. T. Millot, "Submarine hull integrity under blast loading," *Int. J. Impact. Eng.*, vol. 36, no. 8, pp. 1070-1078, 2009.
12. T. P. Nguyen and M. T. Tran, "Response of Vertical Wall Structures under Blast Loading by Dynamic Analysis," *Int. J. Impact. Eng.*, vol. 14, pp. 3308-3316, 2011.
13. M. Godio, *Modelling of masonry walls under seismic loadings*, Paris: Université Paris-Est, 2015.
14. L. Binda and G. Savoia. "Analysis of Masonry Structures under Complex Loading Conditions." *Eng. Struct.*, vol. 24, no. 12, pp. 1599-1610, 2002.
15. P. W. Sielick and T. Łodygowski, "Masonry wall behaviour under explosive loading," *Eng. Fail. Anal.*, vol. 104, pp. 274-291, May 2019.
16. S. Pietruszczak and X. Niu, "A Mathematical Description of Macroscopic Behaviour of Brick Masonry," *Int. J. Solids Struct.*, vol. 29, pp. 531-546, 1992.
17. D. W. Cleary, "Computational Modeling of Masonry Structures: Theoretical and Experimental Aspects." *Computers and Structures*, vol. 88, no. 3, pp. 115-127, 2008.
18. M. Wang, H. Hao and Z. X. Li, Y. Ding, "Prediction of Fragment Size and Ejection Distance of Masonry Wall Under Blast Load Using Homogenized Masonry Material Properties," *Int. J. Impact Eng.*, vol. 36, no. 6, pp. 808-820, 2009.
19. J. P. Tiong, "Analysis of Blast Overpressure and Structural Integrity." *Int. J. Struct. Eng.*, vol. 10, no. 1, pp. 45-59, 2001.
20. H. Draganić and V. Sigmund, "Blast Loading on Structure," *Tehniki vjesnik*, vol. 19, pp. 643-652, 2012.
21. K. Vasilis and S. George, C*alculation of Blast Loads for Application to Structural Components*, Luxembourg: Publications Office of the European Union, 2013.
22. H. Patel, K. C. Panchal and C. S. Jadav, "Structural Analysis of Truck Chassis Frame and Design Optimization for Weight Reduction," *Int. J. Eng. Adv. Tech.*, vol. 2, no. 4, pp. 665-668, 2013.
23. F. Goodnow and M. Zaluzec, "2005 Ford GT - Melding The Past and The Future," *in the SAE 2004 World Congress & Exhibition*, Michigan, United States, 2004.
24. P. Rozylo, "Failure analysis of thin-walled composite structures using independent advanced damage models," *Composite Struct.*, vol. 262, article no. 113598, 2021.
25. X. Yang, Q. Lan and Y. Zhong, "Buckling analysis and experiment of fiber-paper honeycomb sandwich structure composites," *Adv. Mater. Res.*, Vol. 1, pp. 566-570, 2011.